Geophysical Research Letters

RESEARCH LETTER
10.1029/2025GL120802

Leveraging Laboratory Experiments of Shoreline Response to Sea-Level Rise: A Beach Disequilibrium Perspective

M. D'Anna[1,2], F. Ribas[1], G. Coco[3], P. M. Bayle[4], D. Calvete[1], A. Falqués[1], T. E. Baldock[5], A. L. Atkinson[5], and T. Beuzen[6]

[1]Physics Department, Universitat Politecnica de Catalunya, Barcelona, Spain, [2]University of Auckland School of Environment, Auckland, New Zealand, [3]Marine Science Institute (ICM, CSIC), Barcelona, Spain, [4]Faculty of Civil Engineering and GeoSciences, Delft University of Technology, Delft, The Netherlands, [5]School of Engineering, University of Queensland, Brisbane, QLD, Australia, [6]UNSW, School of Civil and Environmental Engineering, Water Research Laboratory, Sydney, NSW, Australia

Abstract This study analyzes laboratory data of beach response to sea-level rise (SLR), isolating shoreline changes driven by passive flooding (PF) of the beach and consequent wave-driven processes. The disequilibrium concept relates shoreline change to instantaneous and equilibrium beach states. While PF shifts the shoreline geometrically, SLR induces disequilibrium that produces wave-driven changes due to apparent profile changes. For the first time, 24 experiments from wave flumes of different scale (including new high-low energy cyclic waves experiments) are gathered into a dimensionless data set through a scaling technique to investigate SLR-induced processes. The data indicate trends (possibly linear) between relative wave power and wave-driven shoreline changes for a given SLR, highlighting the effects of changing background wave energy. Cyclic wave experiments best represent Bruun model's behavior. Wave-energy dissipation emerges as a key variable for quantifying SLR-induced disequilibrium, offering new pathways for future improvements of equilibrium shoreline models under SLR and wave-climate change.

Plain Language Summary This study analyzes the impact of sea-level rise (SLR) on sandy beaches and their shoreline by analyzing laboratory experiments. The analysis separates shoreline changes caused by passive inundation (flooding) from those caused by enhanced wave action. These contributions are interpreted using the concept that given an originally stable beach, SLR disrupts that balance inducing wave-driven changes. For the first time, 24 experiments from wave flumes of different sizes are brought together and converted into a standardized format using a scaling technique, for comparison. The results revealed a possible link between the bulk wave energy dissipation across the beach and the imbalance induced by SLR that drives shoreline changes. However, more experiments are needed to fully understand how waves and SLR together affect the shoreline.

Key Points:

- Wave-driven shoreline response to sea-level rise (SLR) can be related to changes in wave energy dissipation stemming from apparent profile changes
- Flume experiments of different geometric scales can be analyzed together into a non-dimensional data set through a scaling technique
- Cyclic wave and progressive water level change experiments are recommended to emulate the effects of SLR (and fall)

Supporting Information:

Supporting Information may be found in the online version of this article.

Correspondence to:

M. D'Anna,
maurizio.d.anna@upc.edu

Citation:

D'Anna, M., Ribas, F., Coco, G., Bayle, P. M., Calvete, D., Falqués, A., et al. (2026). Leveraging laboratory experiments of shoreline response to sea-level rise: A beach disequilibrium perspective. *Geophysical Research Letters*, *53*, e2025GL120802. https://doi.org/10.1029/2025GL120802

Received 24 NOV 2025
Accepted 22 JAN 2026

Author Contributions:

Conceptualization: M. D'Anna, F. Ribas, G. Coco, D. Calvete, A. Falqués
Data curation: P. M. Bayle, T. E. Baldock, A. L. Atkinson, T. Beuzen
Formal analysis: M. D'Anna
Funding acquisition: M. D'Anna, F. Ribas
Investigation: M. D'Anna, F. Ribas, G. Coco, P. M. Bayle, D. Calvete, A. Falqués
Methodology: M. D'Anna, F. Ribas, G. Coco, P. M. Bayle, D. Calvete, A. Falqués

1. Introduction

Sea-level rise (SLR) is expected to persist globally throughout the current century (Cooley et al., 2022), threatening coastlines worldwide (Cooper & Jackson, 2019) and drawing increasing attention on long-term shoreline predictions. Sandy beaches tend to adapt naturally to SLR with cross-shore changes that depend on interactions among SLR, local processes, availability of sediment and accommodation space (Cooper et al., 2020). However, knowledge gaps in the physically based quantification of beach response to SLR, and the limited duration of available observations (Splinter & Coco, 2021) render the prediction of future shoreline evolution uncertain (Ranasinghe, 2020).

Under persistent sea level and wave conditions, beach profiles are expected to gradually reach a stable equilibrium state (Bruun, 1954). The disequilibrium concept relates the rate of beach changes to the difference between the present beach configuration and its equilibrium state. The approach, corroborated through laboratory (Swart, 1974) and field (Ludka et al., 2015) measurements, can describe wave-driven shoreline change (e.g., Castelle et al., 2014; Jaramillo et al., 2021), or the long-term average migration due to SLR (e.g., Bruun, 1962). SLR impacts beaches and shorelines directly through passive flooding (PF), and indirectly affecting wave propagation and exposing new areas of the beach, enhancing wave-induced erosional potential (Kana et al., 1984). The latter effect can be characterized as a wave-driven response to SLR-induced disequilibrium (D'Anna et al., 2021). According to the equilibrium principle, different wave-water level combinations can be

Resources: F. Ribas, G. Coco, D. Calvete, T. E. Baldock, T. Beuzen
Software: M. D'Anna
Supervision: F. Ribas
Validation: P. M. Bayle
Visualization: M. D'Anna, G. Coco
Writing – original draft: M. D'Anna
Writing – review & editing: F. Ribas, G. Coco, P. M. Bayle, D. Calvete, A. Falqués, T. E. Baldock, A. L. Atkinson

associated with different equilibrium shoreline positions (Miller & Dean, 2004). Variations of waves and/or sea level induce a disequilibrium, triggering morphological changes. In nature, wave conditions continuously change on hourly decadal timescales resulting in complex disequilibrium patterns (D'Anna et al., 2021; Kriebel & Dean, 1985).

Most attempts to explain the effects of SLR assume that the long-term equilibrium beach profile migrates landward to satisfy cross-shore sediment balance (e.g., Dean & Houston, 2016; Luque et al., 2023; McCarroll et al., 2021). The pioneer model adopting this concept is Bruun (1962)'s model, which under specific conditions (e.g., no longshore sediment transport gradients, only offshore sediment transport, no sources/sinks) and assuming an unchanged equilibrium profile shape (i.e., unchanged wave climate), estimates shoreline response to SLR, ΔX_{SLR}, as:

$$\Delta X_{\mathrm{SLR}} = \frac{\mathrm{SLR}}{\tan \alpha} \tag{1}$$

where $\tan \alpha$ is the average beach profile slope between seawards and landward limits of cross-shore sediment transport on the timescale of interest.

These approaches estimate the overall beach profile shift caused by the cumulative effects of SLR, implicitly including the effects of PF and wave-SLR feedback. The importance of explicitly considering the dynamic interactions between waves and water level change is recognized in the literature. For instance, Kriebel and Dean (1985) numerically investigated beach evolution under time-varying storm waves and surges and found that while water levels control the total erosion potential, the associated beach recession is increasingly dependent on the wave height over time. However, also due to the lack of data sets featuring discernible shoreline responses to past SLR, the dynamic wave-SLR feedback remains poorly understood. Observations of Lake Michigan's (USA) shorelines under large interannual water-level fluctuations and moderate waves allowed the explicit modeling of PF and SLR-driven disequilibrium (Abdelhady & Troy, 2023). The model explained past local shoreline changes, but relied on empirical parameters and yet lacks a physical background to quantify the individual contributions to shoreline change.

Laboratory flume physical models of sandy beaches allow us to isolate and investigate morphodynamic processes, reducing the timescale of the associated responses (Hughes, 1993). Recent reduced- (e.g., Atkinson et al., 2018) and prototype-scale (Bayle, Beuzen, et al., 2020; Blenkinsopp et al., 2021) experiments of cross-shore beach response to water level change under steady wave conditions produced ideal data for analyzing wave-SLR feedback. So far, analyses of these data focused on the bulk equilibrium profile migration due to SLR under single stationary wave conditions, and did not explore the individual contributing processes or the effects of varying wave-SLR combination on shoreline change. In addition, raw observations from experiments with different and/or distorted geometric scales can only be compared in terms of qualitative behavior (Van Rijn et al., 2011), preventing a quantitative intercomparison of the data.

Here, we use laboratory data to examine the decomposition of shoreline change induced by SLR on wave-dominated beaches into PF and wave reshaping. Experiments from three different flumes (including a new set of cyclic tests—alternating high/low energy wave conditions) are integrated in a single non-dimensional data set while correcting geometric distortions, using a scaling technique. Finally, we discuss the relationships between SLR and the individual contributions to shoreline change, and compare them with Bruun model estimations.

2. Laboratory Data

Laboratory flume measurements of beach response to SLR are available from three existing physical modeling studies: Atkinson (2018), Beuzen et al. (2018), and Bayle, Beuzen, et al. (2020). These experiments recorded cross-shore beach profile evolution under stationary or cyclic significant wave heights (H_s) and peak periods (T_p), and one or multiple SLR steps, covering a range of waves-SLR combinations. The tests started from prescribed beach profile shapes and allowed waves to drive the profile to quasi-equilibrium before and after the water level step(s). For stationary wave conditions, which can represent either a wave climate or a specific event, the beach profile developed a quasi-static equilibrium shape, and the tests were defined *erosive* or *accretive* when exhibiting a breaker bar or a berm, respectively. Under cyclic wave conditions (periodic fluctuations of H_s and T_p), the

Table 1
Overview of the Experiments Extracted From the Three Data Sets

Data set	ID	Initial slope (–)	Wave type	H_s (m)	T_p (s)	Ω (–)	Pre-SLR depth (m)	SLR (cm)	d_{50} (mm)
Atkinson (2018)	AtkE1	1/10	Pierson-Moskowitz	0.13	1.20	2.71	0.6	6.5	0.28
	AtkE2	1/10	JONSWAP	0.125	1.20	2.60	0.6	6.5	
	AtkE3	2/3-power	JONSWAP	0.125	1.20	2.60	0.6	6.5	
	AtkE4	Final E3	JONSWAP	0.125	1.20	2.60	0.665	−6.5	
	AtkE5	1/15	JONSWAP	0.16	1.18	3.39	0.6	5	
	AtkA1	1/10	Monochromatic	0.05[a]	1.50[a]	1	0.6	5	
	AtkA2	1/10	Monochromatic	0.07[a]	2.00[a]	0.88	0.6	3.5	
	AtkA3	1/10	Pierson-Moskowitz	0.07	2.00	0.88	0.6	3.5	
	AtkC1	Bar-Profile	Pierson-Moskowitz	0.056|0.140	1.00	1.4|3.5	0.6	−3	0.28
	AtkC2	Final C1					0.57	−3	
	AtkC3	Final C2					0.54	3	
	AtkC4	Final C3					0.57	3	
	AtkC5	Final C4					0.6	3	
	AtkC6	Final C5					0.63	3	
Beuzen et al. (2018)	BeuE1	1/15	JONSWAP	0.15	1.25	2.86	1.0	5 × 1.5	0.35
	BeuE2							7.5	
Bayle, Blenkinsopp, et al. (2020)	BayE1	1/15	JONSWAP	0.80	6.00	3.25	4.0	4 × 10	0.33

[a]Note that for monochromatic waves $H_s = H$ and $T_p = T$.

experimental profile achieved a dynamic equilibrium state, rocking between barred and bermed configurations with a stable average position.

The experiments were conducted in flumes with length × depth of 22 × 1 m (Atkinson, *Atk**), 44 × 1.6 m (Beuzen, *Beu**), and 309 × 7 m (Bayle, *Bay**). From the three data sets, we selected 17 experiments (Table 1): single-step SLR under stationary (6 erosive: AtkE1–AtkE5 and BeuE2; 3 accretive: AtkA1–AtkA3) and dynamic (6 cyclic: AtkC1–AtkC6) wave conditions; and incremental SLR with stationary erosive wave conditions (BayE1 and BeuE1). The initial beach profile was a planar slope of 1/10 or 1/15 for 9 experiments, while the rest featured non-linear shapes (e.g., AtkE3) or succeeding previous tests (e.g., AtkC2). The data sets comprise values of SLR relative to the wave height ($|SLR|/H_s$) between 10% (BeuE1) and 100% (AtkA1), including three cases of negative SLR (AtkE4, AtkC1, and AtkC2). The experiments used median grain sizes of 0.28–0.35 mm (sediment fall velocity, w_s, of 0.037–0.044 m/s), resulting in dimensionless fall velocities ($\Omega = H_s/T_p w_s$) of 0.88–3.39.

The individual data sets are further detailed in Text S1 in Supporting Information S1, and experiments used herein are summarized in Table 1.

3. Methods and Data Analysis

3.1. Equilibrium Shoreline Response to SLR

We follow D'Anna et al. (2021)'s interpretation of shoreline response to SLR in absence of sediment sources/sinks and longshore processes. This concept states that as sea level changes, PF drives a geometric shoreline shift and affects the water depth across the beach, altering the original beach-wave disequilibrium. The additional wave-driven shoreline change resulting from this disequilibrium perturbation (named "wave reshaping," WR) is the product of waves interacting with a different morphology (shape) due to sea level change. Wave reshaping results from an apparent steepening/flattening of the nearshore beach profile due to SLR, which reduces/extends the surf-zone and the consequent energy dissipation and sediment transport patterns. This can also be interpreted as a change in wave-driven sediment transport efficiency, or an apparent change of incident wave energy with a possible change in beach state (Baldock et al., 2017; Wright et al., 1985).

While PF can be simply estimated as the projection of SLR on the foreshore slope (tan β):

$$\mathrm{PF} = \frac{\mathrm{SLR}}{\tan\beta} \tag{2}$$

The quantification of WR requires a better understanding of wave-SLR-beach feedback. WR develops gradually over time. Under time-varying wave conditions (as in reality), wave-driven disequilibrium continuously evolves (Yates et al., 2009), so that water level changes result in complex WR patterns, which are superimposed to shoreline changes that would occur without SLR. In this case, WR may develop only partially before a different wave event occurs. Under persistent wave conditions such as those characterizing most of the experiments used here, the cumulative WR evolves with an exponential damping until reaching its maximum at equilibrium with those waves (e.g., Miller & Dean, 2004). When starting from equilibrium conditions, the wave-driven shoreline change following SLR and PF corresponds exactly to WR. The permanent forcing characterizing most of the experiments used here allows to isolate WR and determine the theoretical equilibrium position for different SLR-wave combinations. If the same wave conditions persist for long enough time to attain a new (post-SLR) equilibrium state, this mechanism aligns with the Bruun model.

Here, we quantify WR using simplified experimental settings. In real coastal assessments, local factors such as complex emerged beach topography (Wolinsky & Murray, 2009) or spatial variability of sediment characteristics may affect shoreline trends due to SLR.

3.2. Scaling and Non-Dimensional Data

The current experiments feature different and/or distorted (i.e., different slope) geometric scales. Therefore, quantitative comparisons from different experiments require undistorted scales and a non-dimensional representation of the variables (Van Rijn et al., 2011). To compare shoreline changes from all the experiments into an undistorted dimensionless data set, we adapted Bayle et al. (2021)'s scaling method (BSM) to the present profile (x, z) data. The method is inspired by Peregrine and Williams (2001)' scaling for swash flows, normalizing the non-linear shallow water equations with the nearshore beach slope (m) and a swash-related vertical distance. Such scaling was also previously applied for the dimensional analysis of timescales of beach response to SLR (Kriebel & Dean, 1993). In the BSM, the vertical scaling distance is defined as the maximum wave runup measured during the experiment (R), which relates to the wave conditions and thus to the boundaries of the active beach profile. This leads to the following expression of dimensionless coordinates (x^*, z^*) for any beach slope:

$$x^* = \frac{x\,m}{R}; \qquad z^* = \frac{z}{R} \tag{3}$$

with the (x, z) origin corresponding to the shoreline, defined as the profile intersection with the still water level. Equation 3 normalizes the beach profile slope correcting distortions through m, while R scales the magnitude of measured distances. Here we define m as the initial (pre-SLR equilibrium) slope measured between R and $-R/2$ around the shoreline, which matches the foreshore slope in Equation 2 ($m = \tan\beta$). As the BSM accounts for scale differences between beach models, experiments from the same laboratory are treated as representations of the same beach and are scaled using the same R value: the mean R of the data set. The m and R values measured from each experiment and the mean R for each data set are reported in Table S1 in Supporting Information S1.

The BSM was developed for comparing experimental measurements from different scales and was validated observing similarities in beach responses from three experiments (from the same current data sets) characterized by comparable (erosive) conditions, random waves, and initially planar profiles (Bayle et al., 2021). Here, we apply the method to experiments with differing conditions, including accretive conditions. To test the extended validity of the approach, we verified that the proportions of cross-shore changes between pairs of experiments with the same scale but different conditions are maintained after the scaling (Text S2 in Supporting Information S1).

Scaled hydrodynamic variables are obtained by defining relative sea-level rise (SLR*) and wave power (P^*) as follows:

$$\mathrm{SLR}^* = \frac{\mathrm{SLR}}{H_o}; \qquad P^* = 2\frac{H_o}{L_o}\Omega_o \tag{4}$$

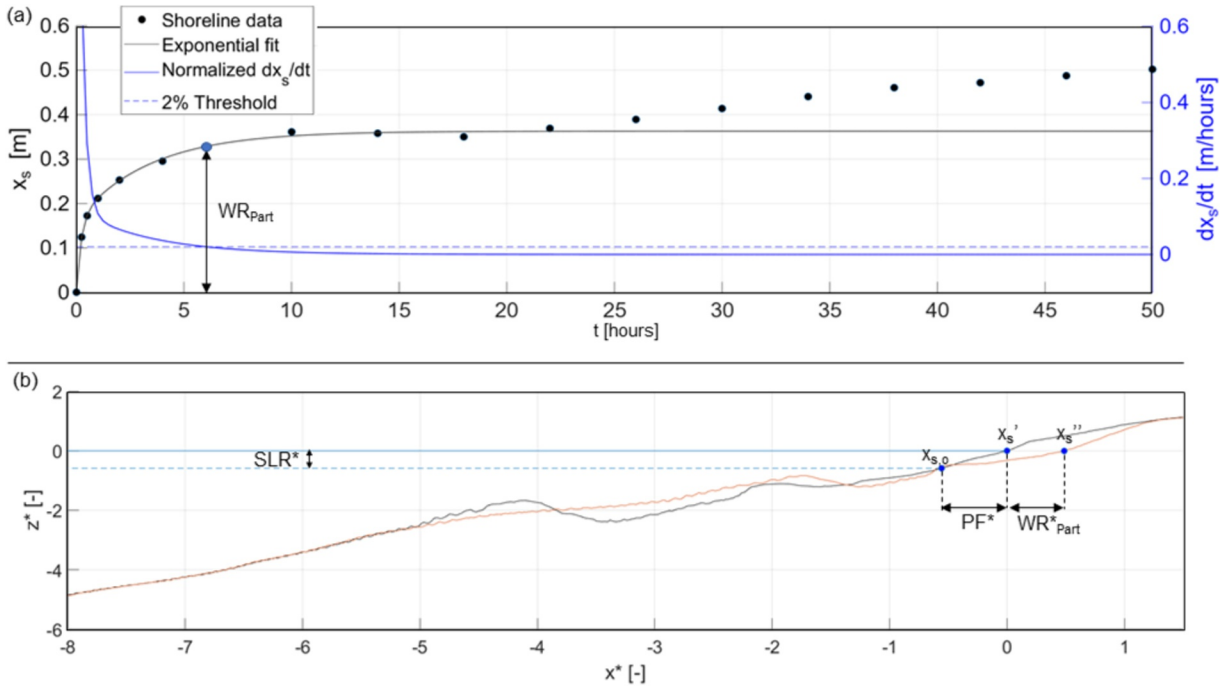

Figure 1. AtkE2 data including: (a) experimental (black dots) and fitted (black line) shoreline evolution and partial wave reshaping (blue circle) corresponding to 2% fitted shoreline change rate (dx_s/dt, blue line on right-hand axis) and (b) initial (black line) and partial (orange line) non-dimensional beach profiles with corresponding PF* and WR^*_{part}.

where H_o and L_o are the wave height and length at the deep-water limit ($d/L = 1/2$), estimated from the corresponding H_s, T_p, and d (Table 1) by reverse linear shoaling; and Ω_o is the dimensionless fall velocity calculated using H_o and L_o. A detailed derivation of Equation 4 is provided in Text S3 in Supporting Information S1. We note that over the ensemble of data, the ratio R/H_o is ≈1 (Figure S2 in Supporting Information S1), which is consistent with existing wave runup formulations (Holman, 1986) or by multi-model fit (Atkinson et al., 2017), considering the current values of m, H_o, and T_p (Table S1 in Supporting Information S1).

3.3. Unifying Data Sets

To better understand shoreline response to SLR we investigate PF and WR under different wave-SLR combinations using the unified experimental data set. For this purpose, we consider multi-step SLR sequences (BeuE1 and BayE1) as ensembles of individual one-step SLR experiments, each starting from the final profile of the previous step. This ensures consistency with the one-step SLR experiments and, since each ensemble member applies the same water-level increment, accounts for some uncertainty on the experiment.

When interpreting the data, we consider the experiments to commence immediately before the application of SLR, with the initial beach profile corresponding to the pre-SLR equilibrium profile. We define the dimensionless shoreline positions (x_s*) as the mean water level intersection with the experimental profiles in the non-dimensional space. The shoreline fluctuations of cyclic tests (AtkC1–AtkC6) are smoothed using a centered moving average (one wave-cycle window), obtaining a mean shoreline position timeseries (Figure S3 in Supporting Information S1).

Typical equilibrium models (e.g., Bruun's) assume a sufficiently slow SLR that results in quasi-instantaneous post-SLR equilibrium. In laboratory settings a static equilibrium state is unlikely achieved (Swart, 1974), and the shoreline position may not stabilize at the end of the experiments (Figure 1a) due to sandbar cycles emerging under random stationary waves (Atkinson, 2018). These issues, further accentuated by the differing timescales of shoreline response under different wave conditions, compromise the comparison of final WRs between different tests. Therefore, we consider the partial WR (WR_{part}) extracted at the time when shoreline change rate reduces to 2% of the rate observed over the first hour of the experiment (Figure 1a, Text S4 in Supporting Information S1).

Such approach ensures that the experiments are compared at a similar morphodynamic stage while accounting for 85%–90% of the total WR (Figure S4 in Supporting Information S1).

For each experiment, we measure (in non-dimensional space) the passive flooding (PF*) and partial wave reshaping (WR^*_{part}) as net shoreline changes (Δx^*) from the scaled beach profiles (Figure 1b), and we analyze them individually with respect to the corresponding SLR* and P^*.

Finally, we compare the Bruun model (Equation 1) estimation with the sum of the dimensional PF and WR, for both the partial and final measured wave reshaping. For the Bruun model application, tan α (between the measured depth of closure and maximum wave runup) is measured on the pre-SLR equilibrium profile, as per the foreshore slope in the BSM application.

4. Results and Discussion

The dimensionless shoreline change contributions (PF* and WR^*_{part}) for the 24 experiments are illustrated in Figure 2 as a function of SLR* and P^*. Overall, the PF* data are linearly related to SLR* (Figure 2a), with no visible correlation with P^* (Figure 2b). Figure 2c shows some correlation between WR^*_{part} and SLR*, reflecting the proportionality of the disequilibrium with SLR*.The data scatter spreads as the magnitude of SLR* increases, which can be explained by the patterns observed in Figure 2d, showing that for SLR* of ∼0.3 and ∼0.5, WR^*_{part} grows with P^*. Therefore, the data suggest that WR^*_{part} increases with P^* for experiment clusters with similar SLR* values and SLR* > 0.1 (Figure 2d), highlighting the role of P^* in determining SLR-driven disequilibrium.

The data associated to the two largest SLR* amplitudes (0.91 and −0.5), which correspond to AtkA1 and AtkE4, diverge notably from the general trends of the data set (Figure 2). For these two experiments, the instantaneous SLR caused the water level to interact with morphological features of the beach (e.g., onshore berm and submerged bar, respectively), resulting in unrealistic PF* and WR^*_{part} (Text S5 and Figure S5 in Supporting Information S1). Therefore, these data are considered outliers.

The dimensionless shoreline changes from cyclic experiments (AtkC1–AtkC6) also align with the general trends of the stationary wave experiment (Figure 2b). While for the same wave conditions this data cluster shows some spreading in WR^*_{part}, we note that the respective experiments were associated to different initial water depths, which influenced wave propagation.

4.1. Passive Flooding and Wave Reshaping

Figure 2a indicates that PF* is mostly dependent on SLR*, consistently with the physics describing PF (Equation 2), and providing further validation to the BSM (Section 4.2). Indeed, given the beach profiles normalization against the linear foreshore slope (Section 3.2), PF* is expected to depend linearly (and solely) on SLR. When removing the two outliers, the linear regression of PF* against SLR* forced through the origin results in a ∼1:1 line (Figure S6 and Table S3 in Supporting Information S1):

$$\frac{PF^*}{SLR^*} \approx 1 \tag{5}$$

consistent with the previous observation that $R/H_o \approx 1$ (Section 3.2).

Figure 2a indicates that for SLR* > 0.3, PF* tend to deviate from the expected linear trend. While PF* values below the trend suggest that some experiments may have not reached a pre-SLR equilibrium, the assumption of a plane foreshore loses validity as SLR increases. The latter occurs for experiments that feature a non-linear shape above the shoreline (as typical equilibrium profiles) and may produce larger PF*. We note that these PF* excesses may also be responsible for the increasing trends observed with P^* in Figure 2b. This suggests that incremental (as opposed to a single-step) SLR experiments are more appropriate to analyze the individual contributions of PF for large SLR.

The increase of WR^*_{part} with SLR* and P^* (Figures 2c and 2d) can be explained by SLR-driven wave energy dissipation changes through non-linear processes (e.g., wave breaking). In fact, recent experimental and numerical works relate bulk wave energy dissipation (D) over fixed impermeable slopes to waves characteristics (H, L), slope angle (β), and water depth (d). Increasing H/L or d/L is found to correspond to higher D through the

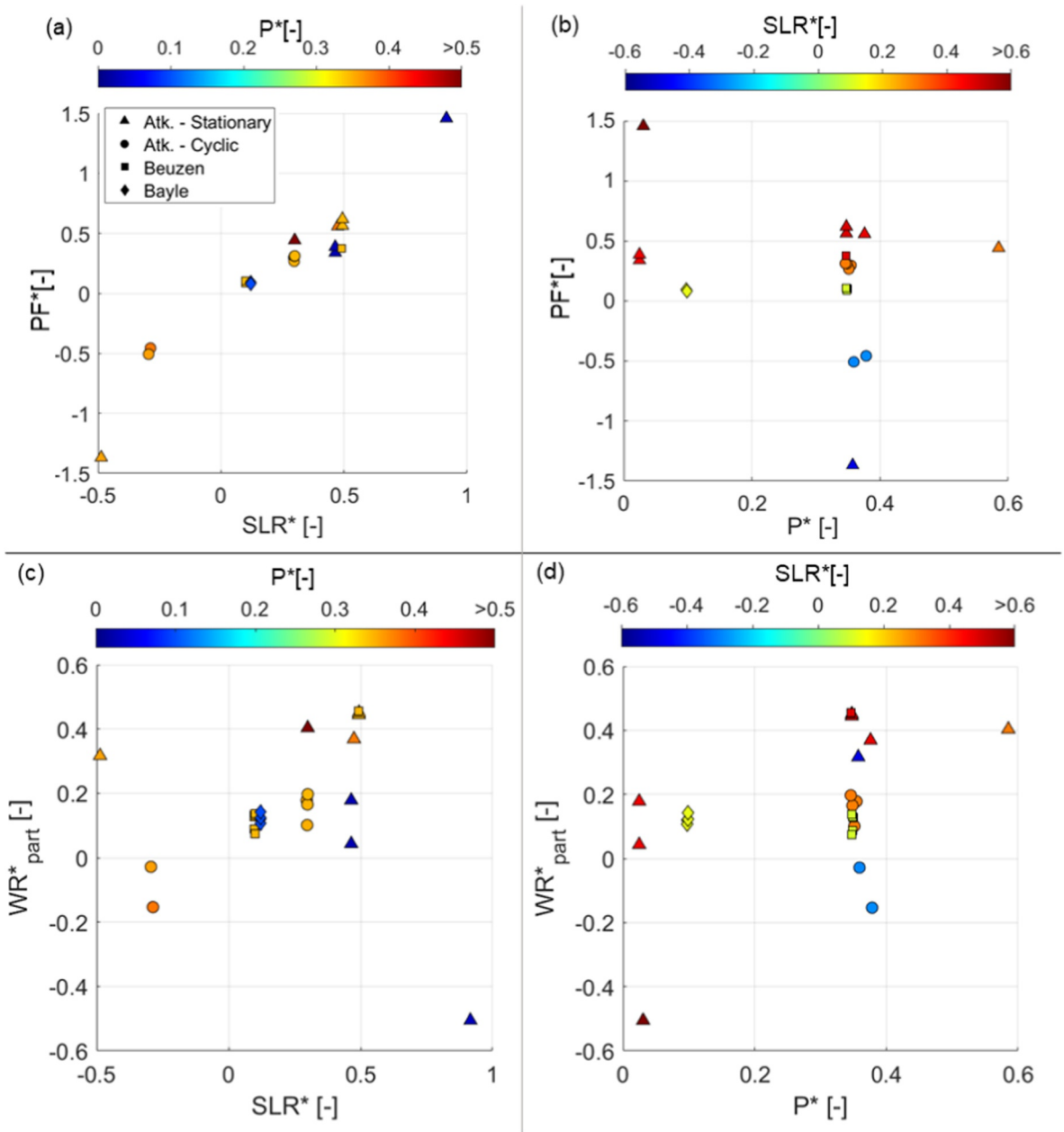

Figure 2. Dimensionless passive flooding (PF*) and partial wave reshaping (WR^*_{part}) against dimensionless (a, c) relative sea-level rise (SLR*) and (b, d) wave power (P^*), for the unified data set. Colourbars of the left and right panels indicate the magnitude of P^* and SLR*, respectively.

surf zone (Díaz-Carrasco et al., 2020) while the dominant wave breaking transitions toward more turbulent types (e.g., from weak to strong plunging waves, Moragues & Losada, 2021). Considering a fixed slope as an initial equilibrium beach profile (with foreshore slope tan β), under the same H and L, an increase of d/L represents an instantaneous SLR. Consistently, Bayle et al. (2021) found that progressive SLR (increasing d/L) over an equilibrium beach profile corresponded to an increase in wave runup and decrease in wave reflection, indicating a transition toward an increasingly dissipative state. This suggests that the instantaneous (positive or negative) SLR-induced disequilibrium driving WR^*_{part} can be related to changes in D arising from an apparent change of bottom profile, along the lines of Kriebel and Dean (1993). For a given d/L (representing post-SLR depth), D also increases with H/L, consistently with the underlying principle of wave-driven shoreline models (e.g., Davidson et al., 2013). Therefore, while the current data set is not sufficient to derive a functional relationship between WR^*_{part}, SLR*, and P^*, the wave reshaping effect can be integrated into equilibrium shoreline models by relating

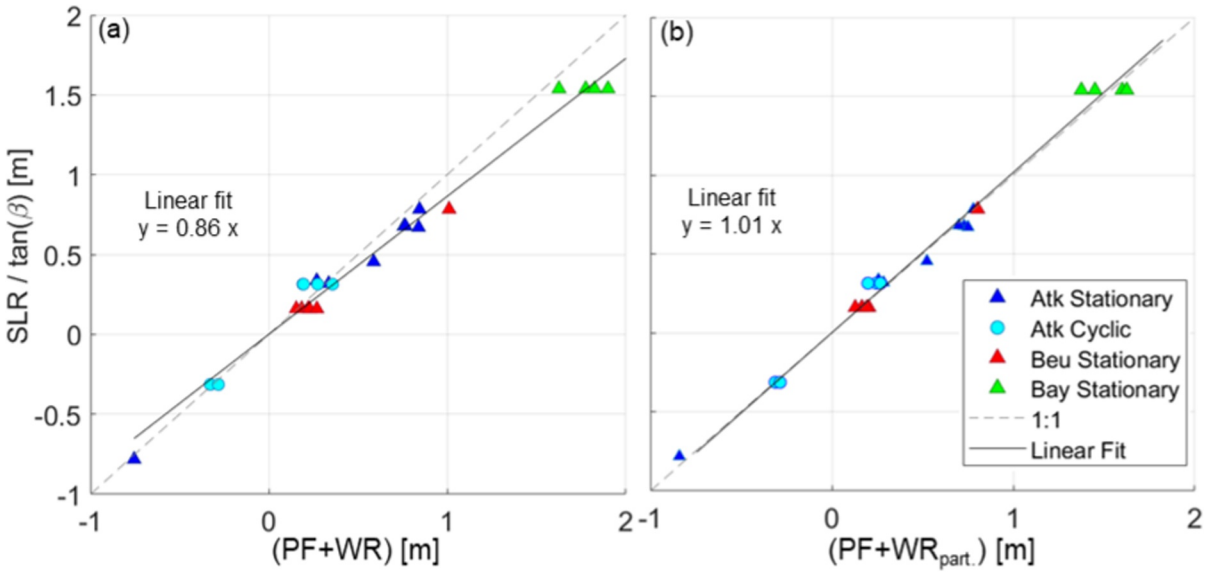

Figure 3. Dimensional shoreline change against Bruun model estimations, for (a) final and (b) partial wave reshaping, including stationary (triangles) and cyclic (circles) experiments for the unified data set, with respective least squares fit (solid line).

SLR-induced disequilibrium to D. Such relationships could be derived analytically through energy flux conservation and equilibrium beach theory (Dean, 1977; Kriebel & Dean, 1985), similarly to previous attempts made for wave-driven beach evolution models (Birrien & Baldock, 2021).

Given the equilibrium-based design underlying the experiments, the total shoreline change (PF + WR) is expected to follow the Bruun response (D'Anna et al., 2021). As the Bruun model depends on the mean beach slope and PF on the foreshore slope, WR/PF depends on the mean beach slope at equilibrium, which is linked to the wave power and Ω (i.e., P^*). While the data (including the outliers) confirm this behavior, the Bruun model appears to underestimate shoreline change for stationary erosive experiments (Figure 3a), in agreement with Atkinson et al. (2018). The data better fit the Bruun model when considering WR_{part} (Figure 3b). This is likely due to residual shoreline trends produced by the sandbar dynamics (Atkinson et al., 2018; Baldock et al., 2017), but also to the application of single-step instead of a slow continuous SLR (Bayle et al., 2021). Cyclic experiments reach a dynamic equilibrium with no hysteretic changes (Baldock et al., 2017) and better align with the Bruun model, suggesting that this type of experiment is more appropriate to test equilibrium-based models. Contrary to its own assumptions, the Bruun model also agrees with the experimental data for negative SLR. While this appears to validate the model, the data agreement is favored by the controlled experimental setup. In nature, Bruun's model has been observed to fail under negative SLR, due to the timescale of onshore-directed processes (longer than offshore-directed) and sediment budget and equilibrium profile conservation (e.g., Enayatighadikolaei et al., 2025).

4.2. Implications for Extended Scaling Method

The scatter plots in Figure 2 show consistent results from experiments of different data sets with similar hydrodynamics (e.g., SLR* ∼ 0.1 and ∼0.5, or P^* ∼ 0. 35). In addition, the experimental data are well distributed along the line describing PF* versus SLR* (Figure 2a), regardless of the experiment source and scale. These results, along with the quantitative verification of the scaling (Section 3.2), extend the validation of BSM for comparing shoreline change from experiments characterized by different hydrodynamics, including cases dominated by accretive processes, monochromatic waves and non-planar initial profiles. The results also indicates that multi-step SLR experiments can be treated as repetition of one-step SLR cases, overcoming some limitations found in the previous comparison of AtkE5, BeuE1, and BayE1 from Bayle et al. (2021).

5. Conclusions

For the first time, 24 experiments from wave flumes of different scale are successfully gathered into a unified dimensionless data set to investigate SLR-induced processes. The data highlight the different nature of PF and wave reshaping, and the feedback among beach profile, SLR and wave energy dissipation. Passive flooding is controlled by SLR and the equilibrium beach foreshore slope, following the expected behavior. Wave reshaping trends with SLR and wave power are consistent with wave energy dissipation changes observed in previous studies for varying water levels, suggesting that SLR-induced disequilibrium can be quantified in terms of bulk energy dissipation. These findings support future approaches for integrating SLR into equilibrium shoreline models while resolving wave-SLR feedback (wave reshaping) explicitly, which is critical in the context of future wave climate change. However, further data is required to derive statistically robust relationships and characterize wave reshaping, or analytical expressions linking SLR-induced disequilibrium to wave energy dissipation. The individual total shoreline responses, combining PF and wave reshaping, align with the Bruun model, providing an explicit physical background to the model when the conceptual assumptions are satisfied. Limitations in applying single-step water level increases and/or stationary wave conditions advocate that future laboratory tests should enforce realistic gradual SLR under cyclic wave conditions to represent the dynamic equilibrium modeled in typical volume conservation approaches (e.g., Bruun). The results support the innovative application of scaling techniques for unifying data from experiments with substantially different geometric scales and wave conditions into a single (non-dimensional) data set.

Conflict of Interest

The authors declare no conflicts of interest relevant to this study.

Data Availability Statement

Data and codes generated during this work are accessible on the following online repository: D'Anna (2025).

Original laboratory data are detailed in Atkinson et al. (2018), Beuzen et al. (2018), and Blenkinsopp et al. (2021), and are available upon request or to download from Schimmels and Blenkinsopp (2020).

Acknowledgments

M. D. funded by the European Union HORIZON research and innovation program under the MSCA (101107336); F. R., D. C., and A.F. supported by PID2021-124272OB-C22 and PID2024-157818OB-C21, funded by the Spanish government MCIN/AEI/10.13039/501100011033/ and by "ERDF A way of making Europe"; G. C. funded by the "Our Changing Coast Project" (MBIE-NZ RTVU2206); T. Be by Australian Research Council Discovery (DP140101302). We thank the three anonimous reviewers for their constructive comments that improved the clarity of this work.

References

Abdelhady, H. U., & Troy, C. D. (2023). A reduced-complexity shoreline model for coastal areas with large water level fluctuations. *Coastal Engineering*, *179*, 104249. https://doi.org/10.1016/j.coastaleng.2022.104249

Atkinson, A. L. (2018). *Laboratory beach profile dynamics and responses to changing water levels with and without nourishment school of civil engineering*. University of Queensland.

Atkinson, A. L., Baldock, T. E., Birrien, F., Callaghan, D. P., Nielsen, P., Beuzen, T., et al. (2018). Laboratory investigation of the Bruun Rule and beach response to sea level rise. *Coastal Engineering*, *136*, 183–202. https://doi.org/10.1016/j.coastaleng.2018.03.003

Atkinson, A. L., Power, H. E., Moura, T., Hammond, T., Callaghan, D. P., & Baldock, T. E. (2017). Assessment of runup predictions by empirical models on non-truncated beaches on the south-east Australian coast. *Coastal Engineering*, *119*, 15–31. https://doi.org/10.1016/j.coastaleng.2016.10.001

Baldock, T. E., Birrien, F., Atkinson, A., Shimamoto, T., Wu, S., Callaghan, D. P., & Nielsen, P. (2017). Morphological hysteresis in the evolution of beach profiles under sequences of wave climates - Part 1; observations. *Coastal Engineering*, *128*, 92–105. https://doi.org/10.1016/j.coastaleng.2017.08.005

Bayle, P. M., Beuzen, T., Blenkinsopp, C. E., Baldock, T. E., & Turner, I. L. (2020). Beach profile changes under sea level rise in laboratory flume experiments at different scale. *Journal of Coastal Research*, *95*(sp1), 192. https://doi.org/10.2112/SI95-038.1

Bayle, P. M., Beuzen, T., Blenkinsopp, C. E., Baldock, T. E., & Turner, I. L. (2021). A new approach for scaling beach profile evolution and sediment transport rates in distorted laboratory models. *Coastal Engineering*, *163*, 103794. https://doi.org/10.1016/j.coastaleng.2020.103794

Bayle, P. M., Blenkinsopp, C. E., Conley, D., Masselink, G., Beuzen, T., & Almar, R. (2020). Performance of a dynamic cobble berm revetment for coastal protection, under increasing water level. *Coastal Engineering*, *159*, 103712. https://doi.org/10.1016/j.coastaleng.2020.103712

Beuzen, T., Turner, I. L., Blenkinsopp, C. E., Atkinson, A., Flocard, F., & Baldock, T. E. (2018). Physical model study of beach profile evolution by sea level rise in the presence of seawalls. *Coastal Engineering*, *136*, 172–182. https://doi.org/10.1016/j.coastaleng.2017.12.002

Birrien, F., & Baldock, T. (2021). A coupled hydrodynamic-equilibrium type beach profile evolution model. *Journal of Marine Science and Engineering*, *9*(4), 353. https://doi.org/10.3390/jmse9040353

Blenkinsopp, C. E., Bayle, P. M., Conley, D. C., Masselink, G., Gulson, E., Kelly, I., et al. (2021). High-resolution, large-scale laboratory measurements of a sandy beach and dynamic cobble berm revetment. *Scientific Data*, *8*(1), 22. https://doi.org/10.1038/s41597-021-00805-1

Bruun, P. (1954). Coast erosion and the development of beach profiles. In *Technical memorandum No. 44, beach erosion board*.

Bruun, P. (1962). Sea-level rise as a cause of shore erosion. *Journal of the Waterways and Harbors Division*.

Castelle, B., Marieu, V., Bujan, S., Ferreira, S., Parisot, J.-P., Capo, S., et al. (2014). Equilibrium shoreline modelling of a high-energy meso-macrotidal multiple-barred beach. *Marine Geology*, *347*, 85–94. https://doi.org/10.1016/j.margeo.2013.11.003

Cooley, S., Schoeman, D., Bopp, L., Boyd, P., Donner, S., Ito, S. I., et al. (2022). Oceans and coastal ecosystems and their services. In *Climate change 2022: Impacts, adaptation and vulnerability. Contribution of the WGII to the 6th assessment report of the intergovernmental panel on*

climate change. IPCC AR6 WGII. Retrieved from https://www.ipcc.ch/report/ar6/wg2/downloads/report/IPCC_AR6_WGII_FinalDraft_Chapter03.pdf

Cooper, J. A. G., & Jackson, D. W. T. (2019). Coasts in peril? A shoreline health perspective. *Frontiers in Earth Science*, *7*, 260. https://doi.org/10.3389/feart.2019.00260

Cooper, J. A. G., Masselink, G., Coco, G., Short, A. D., Castelle, B., Rogers, K., et al. (2020). Sandy beaches can survive sea-level rise. *Nature Climate Change*, *10*(11), 993–995. https://doi.org/10.1038/s41558-020-00934-2

D'Anna, M. (2025). Leveraging laboratory experiments of shoreline response to sea-level rise: A beach disequilibrium perspective [Dataset]. *Zenodo*. https://doi.org/10.5281/zenodo.16753126

D'Anna, M., Idier, D., Castelle, B., Vitousek, S., & Le Cozannet, G. (2021). Reinterpreting the Bruun Rule in the context of equilibrium shoreline models. *Journal of Marine Science and Engineering*, *9*(9), 974. https://doi.org/10.3390/jmse9090974

Davidson, M. A., Splinter, K. D., & Turner, I. L. (2013). A simple equilibrium model for predicting shoreline change. *Coastal Engineering*, *73*, 191–202. https://doi.org/10.1016/j.coastaleng.2012.11.002

Dean, R. G. (1977). Equilibrium beach profiles: U.S. Atlantic and Gulf coasts.

Dean, R. G., & Houston, J. R. (2016). Determining shoreline response to sea level rise. *Coastal Engineering*, *114*, 1–8. https://doi.org/10.1016/j.coastaleng.2016.03.009

Díaz-Carrasco, P., Moragues, M. V., Clavero, M., & Losada, M. Á. (2020). 2D water-wave interaction with permeable and impermeable slopes: Dimensional analysis and experimental overview. *Coastal Engineering*, *158*, 103682. https://doi.org/10.1016/j.coastaleng.2020.103682

Enayatighadikolaei, H., Suzuki, T., Soltanpour, M., & Thilakarathne, S. (2025). Application of the Bruun Rule in evaluating the effect of water level fall on the Caspian Sea profile evolution. *Coastal Engineering Journal*, *67*(1), 181–195. https://doi.org/10.1080/21664250.2024.2422167

Holman, R. A. (1986). Extreme value statistics for wave run-up on a natural beach. *Coastal Engineering*, *9*(6), 527–544. https://doi.org/10.1016/0378-3839(86)90002-5

Hughes, S. A. (1993). *Physical models and laboratory techniques in coastal engineering* (Vol. 7). World Scientific. https://doi.org/10.1142/2154

Jaramillo, C., González, M., Medina, R., & Turki, I. (2021). An equilibrium-based shoreline rotation model. *Coastal Engineering*, *163*, 103789. https://doi.org/10.1016/j.coastaleng.2020.103789

Kana, T. W., Michel, J., Hayes, M. O., & Jensen, J. R. (1984). The physical impact of sea level rise in the area of Charleston, South Carolina. In *Greenhouse effect and sea level rise* (pp. 105–150). Springer US. https://doi.org/10.1007/978-1-4684-6569-3_4

Kriebel, D. L., & Dean, R. G. (1985). Numerical simulation of time-dependent beach and dune erosion. *Coastal Engineering*, *9*(3), 221–245. https://doi.org/10.1016/0378-3839(85)90009-2

Kriebel, D. L., & Dean, R. G. (1993). Convolution method for time-dependent beach-profile response. *Journal of Waterway, Port, Coastal, and Ocean Engineering*, *119*(2), 204–226. https://doi.org/10.1061/(ASCE)0733-950X(1993)119:2(204)

Ludka, B. C., Guza, R. T., O'Reilly, W. C., & Yates, M. L. (2015). Field evidence of beach profile evolution toward equilibrium. *Journal of Geophysical Research: Oceans*, *120*(11), 7574–7597. https://doi.org/10.1002/2015JC010893

Luque, P., Gómez-Pujol, L., Ribas, F., Falqués, A., Marcos, M., & Orfila, A. (2023). Shoreline response to sea-level rise according to equilibrium beach profiles. *Scientific Reports*, *13*(1), 15789. https://doi.org/10.1038/s41598-023-42672-3

McCarroll, R. J., Masselink, G., Valiente, N. G., Scott, T., Wiggins, M., Kirby, J.-A., & Davidson, M. A. (2021). A rules-based shoreface translation and sediment budgeting tool for estimating coastal change: ShoreTrans. *Marine Geology*, *435*, 106466. https://doi.org/10.1016/j.margeo.2021.106466

Miller, J. K., & Dean, R. G. (2004). A simple new shoreline change model. *Coastal Engineering*, *51*(7), 531–556. https://doi.org/10.1016/j.coastaleng.2004.05.006

Moragues, M. V., & Losada, M. Á. (2021). Progression of wave breaker types on a plane impermeable slope, depending on experimental design. *Journal of Geophysical Research: Oceans*, *126*(5), e2021JC017211. https://doi.org/10.1029/2021JC017211

Peregrine, D. H., & Williams, S. M. (2001). Swash overtopping a truncated plane beach. *Journal of Fluid Mechanics*, *440*, 391–399. https://doi.org/10.1017/S002211200100492X

Ranasinghe, R. (2020). On the need for a new generation of coastal change models for the 21st century. *Scientific Reports*, *10*(1), 2010. https://doi.org/10.1038/s41598-020-58376-x

Schimmels, S., & Blenkinsopp, C. (2020). DynaRev - Dynamic coastal protection: Resilience of dynamic revetments under sea level rise (Scientific Data - Processed Dataset) [Dataset]. *Zenodo*. https://doi.org/10.5281/ZENODO.3889796

Splinter, K. D., & Coco, G. (2021). Challenges and opportunities in coastal shoreline prediction. *Frontiers in Marine Science*, *8*. https://doi.org/10.3389/fmars.2021.788657

Swart, D. H. (1974). *Offshore sediment transport and equilibrium beach profiles*. TU Delft.

Van Rijn, L. C., Tonnon, P. K., Sánchez-Arcilla, A., Cáceres, I., & Grüne, J. (2011). Scaling laws for beach and dune erosion processes. *Coastal Engineering*, *58*(7), 623–636. https://doi.org/10.1016/j.coastaleng.2011.01.008

Wolinsky, M. A., & Murray, A. B. (2009). A unifying framework for shoreline migration: 2. Application to wave-dominated coasts. *Journal of Geophysical Research*, *114*(F1), F01009. https://doi.org/10.1029/2007JF000856

Wright, L. D., Short, A. D., & Green, M. O. (1985). Short-term changes in the morphodynamic states of beaches and surf zones: An empirical predictive model. *Marine Geology*, *62*(3–4), 339–364. https://doi.org/10.1016/0025-3227(85)90123-9

Yates, M. L., Guza, R. T., & O'Reilly, W. C. (2009). Equilibrium shoreline response: Observations and modeling. *Journal of Geophysical Research*, *114*(C9), C09014. https://doi.org/10.1029/2009JC005359